# A Wavelet Method to Solve High-dimensional Transport Equations in Semiconductor Devices

Vincent Peikert and Andreas Schenk
Integrated Systems Laboratory
ETH Zurich, Switzerland
Email: vpeikert@iis.ee.ethz.ch

***Abstract*—The Multi-Wavelet (MW) Discontinuous Galerkin method (DG) (MWDG) for high polynomial orders (POs) is proposed for the solution of 6-dimensional transport equations for the first time. In contrast to the popular Spherical Harmonics expansion method (SHE), the DG formulation is stable under the application of high order piecewise polynomials (pp) in energy and real space dimensions which turn out to clearly outperform piecewise constants (pc). MWs build a hierarchical basis for all piecewise polynomials (pps) so that the MWDG and the usual nodal DG (NDG) can be equivalent. However, in the MWDG it is possible to reduce the problem to small adaptively compressed sub spaces which strongly reduces the computational costs at only a small expense of accuracy. The increasing TCAD challenges for the simulation of new 3-dimensional nano-devices could be approached by efficient MWDG Boltzmann and Wigner solvers.**

## I. Introduction

Recently, wavelets have been proposed as basis functions for the solution of 6-dimensional semiconductor transport equations (Boltzmann Transport Equation (BTE), Wigner Equation) for the first time [1]. The main advantage of wavelets are their hierarchical compression and adaptation properties enabling an adaptive solution with a fraction of the coefficients that are necessary with a conventional basis. Since the advantages of wavelets increase in higher dimensions, they could enable uniquely accurate TCAD tools for 2- and (with strongly growing importance) 3-dimensional devices. Hence, in [1] the MWDG has been proposed and shown to reduce the number of coefficients by about 99 % with pc MWs. As a next step and in order to further reduce the coefficients, the MWDG for high polynomial orders (POs) is demonstrated in this work for the first time.

## II. The MWDG Method

The DG method has been proposed for the solution of the BTE recently in [5]. The DG method allows for adaptive $hp-$refinement in all coordinates, is flux conserving and stable and is therefore a promising alternative for the established SHE (see e.g. [8]). As basis functions for the DG, pp on (unstructured) meshes are used. To keep the notation simple, let $V_n^k$ be the space of all one-dimensional pp of the degree less than $k$ on a uniform mesh with $2^n$ equidistant intervals within $[0,1]$. By bisecting the mesh, pp build a dense basis in $L_2$ and fulfill the following nested structure:

$$V_0^k \subset V_1^k ... \subset V_n^k ... \subset L_2([0,1]). \tag{1}$$

It is possible to decompose $V_{n+1}^k$ into $V_n^k$ and a perpendicular space $W_n^k$ which only contains the additional details of $V_{n+1}^k$ compared to $V_n^k$ and is therefore be referred to as a detail space

$$V_n^k \oplus W_n^k = V_{n+1}^k, \qquad V_n^k \perp W_n^k. \tag{2}$$

Recursively, $V_n^k$ can be decomposed by detail spaces

$$V_n^k = V_0^k \oplus W_0^k \oplus W_1^k \oplus ... \oplus W_{n-1}^k. \tag{3}$$

$W_l^k$ is spanned by $2^{l-1}k$ detail functions $\psi_{l,i,j}$ called MWs (see [2]) where $l$ indexes the detail order, $j$ indexes the vanishing moment order and $i$ indexes the position. All $\psi_{l,i,j}$ for a position and a detail are shifted and scaled children of one mother wavelet $\psi_j$. $V_0^k$ in (3) are chosen to be the Legendre polynomials in this work.

Instead of using pp $\in V_n^k$ (NDG), the solution of the BTE $\Phi$ is expanded in multi-dimensional MWs basis (MWDG) constructed by tensor products of one-dimensional basis (the wavelet are indexes by multi-indexes for simplicity):

$$\Phi(x,y,z,\mu,\phi,\omega) = \sum_{i,j,k,l} \alpha_{i,j,k,l} \psi_i^{x,y,z} \psi_j^{\mu} \psi_k^{\phi} \psi_l^{\omega}, \tag{4}$$

where x,y,z are the real space coordinates, $\mu$ is the cosine of the polar angle, $\phi$ is the azimuthal angle and $\omega$ is the energy. A tensor product construction is only build within the momentum space and with the real space. Within the real space unstructured grids are typically necessary and the construction of MWs $\psi^{x,y,z}$ on unstructured grids can be done following the procedure in [3]. A strongly growing community utilizes wavelets (and other hierarchical bases) for adaptive compressions. For the solution of PDEs, hierarchical bases build the driving force behind modern adaptive solvers and pre-conditioners. However, of particular interest are the properties of high-dimensional wavelet tensor bases (such as (4)). Due to the orthonormality and the hierarchical property of MWs the norm equivalence

$$\left(|\Phi(x,y,z,\mu,\phi,\omega)|_{L_2}\right)^2 = \sum \alpha_{i,j,k,l}^2 \tag{5}$$

holds and the coefficients $\alpha_{i,j,k,l}$ decay with the detail order. The coefficient decay is strongly enhanced in multi-dimensional tensor bases so that most wavelets can be canceled. This is referred to as high-dimensional wavelets compression (HWC) here and is called adaptive sparse grids in literature (see [6]). Preliminary work about adaptive sparse grids concentrated on FEM formulations and on scalar wavelets rather then on the flux conserving formulations that are necessary for the solution of transport equations. In contrast to scalar wavelets, MWs have an additional vanishing moment hierarchy within each detail to represent high order pp and compression leads to some kind of super sparse grid. This is referred to as vanishing moment compression (VMC) here. Preliminary work on DG and MWs (see e.g. [4]) use MW coefficients as adaption criterion but always keep a full grid so that the MWDG and the NDG stay equivalent. This is referred to as ordinary wavelet compression (OWC) in this work. The effects of HWC have been studied in [1] already. In this work, the additional advantages of higher POs and VMC are analyzed. The proof of principle for the uncompressed and the compressed high PO MWDG method as well as a fair comparison between different POs (here for the orders 0,1, and 3) in all dimensions is presented.

## III. High PO MWDG Performance Study

### A. Bulk Case

*1) Study Description:* Insights about the behavior of the adaptive MWDG in the momentum space can be gained by applying bulk silicon simulations with different numbers of invested degrees of freedom (DOF). For the smooth bulk solutions the $L_2$ norm is a decent error criterion, so that simply the absolute coefficient values are chosen as adaption criterion (see Eq. (5)). The MWDG can fairly be compared to an adaptive NDG: for the NDG the MW adaption has simply to be constrained such that a full grid is ensured at all times (OWC). Additionally, a comparison with a state-of the art SHE method proposed in [8] (and which had been released by SYNOPSYS as a commercial TCAD tool [9]) is done. For the SHE simulations, the mesh is coarsened only uniformly since (to the best knowledge of the authors) non-uniform energy meshes have not been applied for the SHE method so far. As a reference, Monte Carlo simulations are performed with the SYNOPSYS Monte Carlo simulator SPARTA.

*2) Study Results:* In the bulk case, SH reduce to the Legendre polynomials (LP). However, LP in $\mu$ and pc in $\omega$ direction is only a special case of the bases used for the NDG and the MWDG. Fig. 1 compares the drift velocities in dependence of the electric field for the SHE and the DG formulations for different uniform meshes. For both, the same 4th order LP in $\mu$ and pc in energy direction are used. The DG formulation shows superior behavior under mesh coarsening compared to the SHE formulation. Whereas the DG simulation with 16 grid points has acceptable accuracy, the SHE method requires 32 grid points. It seems that the staggered grid approach of the SHE is more sensitive under strong coarsening. Fig. 2 compares the relative (drift velocity)

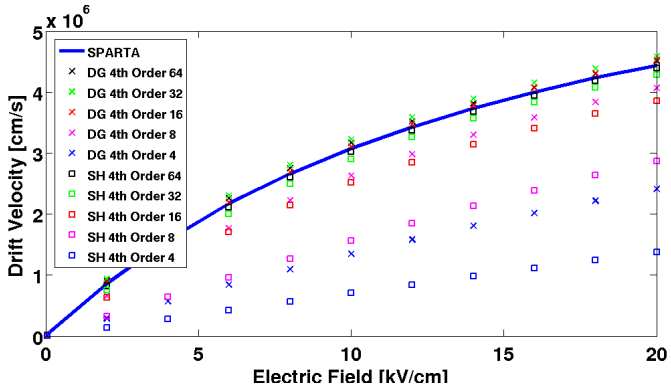


Fig. 1. The Fig. compares the performance of the SHE and the DG formulations in bulk silicon for different energy meshes.

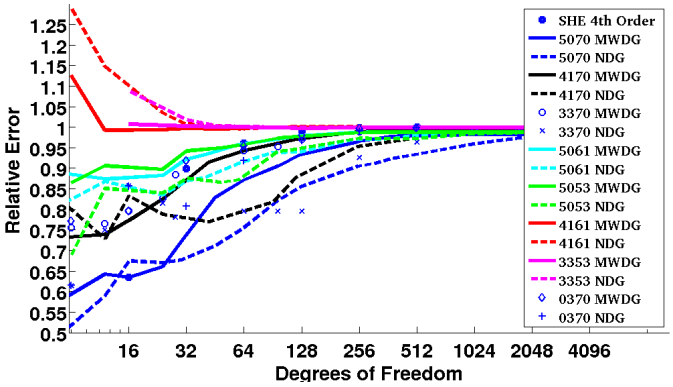


Fig. 2. The Fig. draws the relative errors of the drift velocity at $E = 80\frac{V}{cm}$ in dependence of the number the DOF in MWDG, NDG and SHE simulations.

errors of the adaptive MWDG, NDG and the uniform mesh SHE solutions at $E = 80\frac{kV}{cm}$ with different number of DOF. The high PO simulations in "3353" (maximum number of mesh cells in $\mu$: $2^3$, PO in $\mu$: 3, maximum number of mesh cells in $\omega$: $2^5$, PO in $\omega$: 3) and "4161" strongly outperform the low PO simulations. The application of high PO in $\omega$ direction is valuable. For the adaptive NDG method only between 32 and 48 DOF are necessary to meet a 1 % error criterion whereas the SHE method requires 128 DOF. The corresponding MWDG simulations only require 16 DOF to meet the same error criterion so that the VMC and HWC additionally compress by 50 %. Figure 2 shows the MWDG "3353" solution with 16 DOF compared to the solution with 4096 DOF.

### B. Device Case

*1) Study Description:* First, a grid for the uncompressed 0th order MWDG with 66,304 coefficients is created by careful manual adaptation. From that the grids for higher POs are naively generated by directly replacing grid points with high polynomial order so that the coefficient density stays the same everywhere in the phase space. Finally, the solutions are compressed to 6000 coefficients and solved by MWDG. The same well-studied $n+nn^+$ structure as in [1] is simulated and

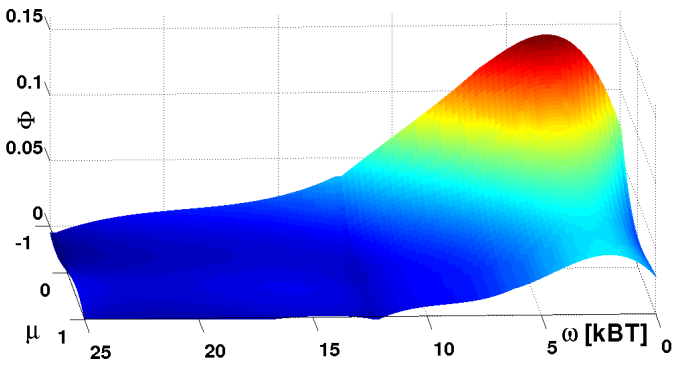


Fig. 3. The Fig. shows the "3353 MWDG" bulk solution from Fig. 2 with 16 MWs.

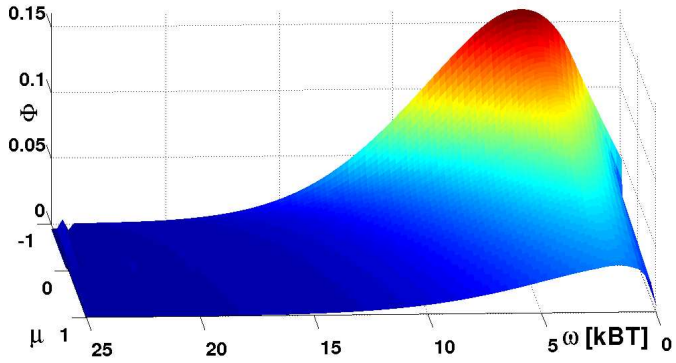


Fig. 4. The Fig. shows the "3353 MWDG" bulk solution from Fig. 2 with 4096 MWs.

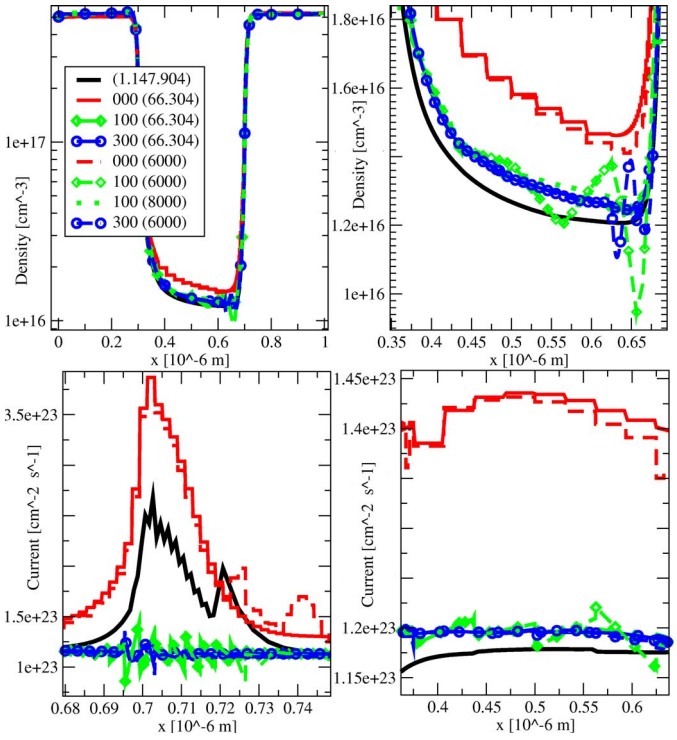


Fig. 5. $n^+nn^+$ simulations at 1V drain with high POs in x direction. Note: The shown currents are not the upwinding fluxes (which would be conserved), but calculated from the solutions of the BTE $\Phi$ directly.

the same well-benchmarked uncompressed 0th PO MWDG simulation with 1,147,904 coefficients as in [1] is used as a benchmark reference.

*2) Study Results:* Figs. 5 and 6 show that the uncompressed MWDG is stable with all POs (no spurious oscillations, distribution function $\Phi$ is positive). All high-order simulations perform significantly better than the 0th order in both, density and current. Surprisingly, the high-order $x$ simulations "100" (PO in $x$: 1, PO in $\mu$: 0, PO in $\omega$: 0)) and "300" perform best: At $x = 0.5$ the 000 error in the current is 21.3 %, whereas the 100 and 300 errors are only 1.47 %. Furthermore, since the discontinuities of the solutions within the $n^+n$ junctions are strongly suppressed, the over-estimations of the currents within the $n^+n$ regions (which appear in all upwinding formulations for the BTE) are strongly reduced. The high $\omega$ orders 013 and 033 show the second best behavior (5.88 % error both), whereas the high $\mu$ orders 011 and 031 are not acceptable (12.5 % error). For adaptive compression, $\Phi$ should be decomposed in $\Phi = \Phi_E + \Phi_V$ . $\Phi_E$ lives on a subspace composing all MWs that are constant in $\mu$ direction and containing the energy and density information. The energy is a density normed quantity. Hence, the contribution of the wavelets to the norm $|\frac{\Phi_E}{n}|_{L_2}$ should be chosen as adaptation criterion. $\Phi_E$ contains steep gradients so that thresholds should be chosen carefully (Fig. 7). $\Phi_V$, on the other hand, contains i.a. the current information. Since the current is of absolute relevance, the contribution of the wavelets to the norm $|\Phi_V|_{L_2}$ should be chosen. Consequently, high compression rates are possible for $\Phi_V$. Following these new adaptation rules, in Figs. 1 and 2 $\Phi_E$ is compressed to 1000 DOF (from 4736) and $\Phi_V$ is compressed to 5000 DOFs (from 61,568). The compression of high-order $\mu$,$\omega$ MWDG performs well so that over 90 % compression is possible without much loss of accuracy (Figs. 6 and 8). However, the compressions for high $x$ orders show local inaccuracies in the density. Applying 8000 coefficients (Fig. 6) or improved current weighted adaptation rules can already solve that problem.

## IV. Conclusion

High-order polynomials perform significantly better than piecewise constants for uncompressed MWDG (up to 96% DOF saving for only 1.4% error in the current). A new wavelet compression rule applying a phase space separation can compress the solution additionally by over 90 %. Even larger compression rates are expected for future full hp-adaptive MWDG simulations in 6-dimensional phase spaces.

## Acknowledgment

Partial funding of this project by Toshiba Corporation is gratefully acknowledged.

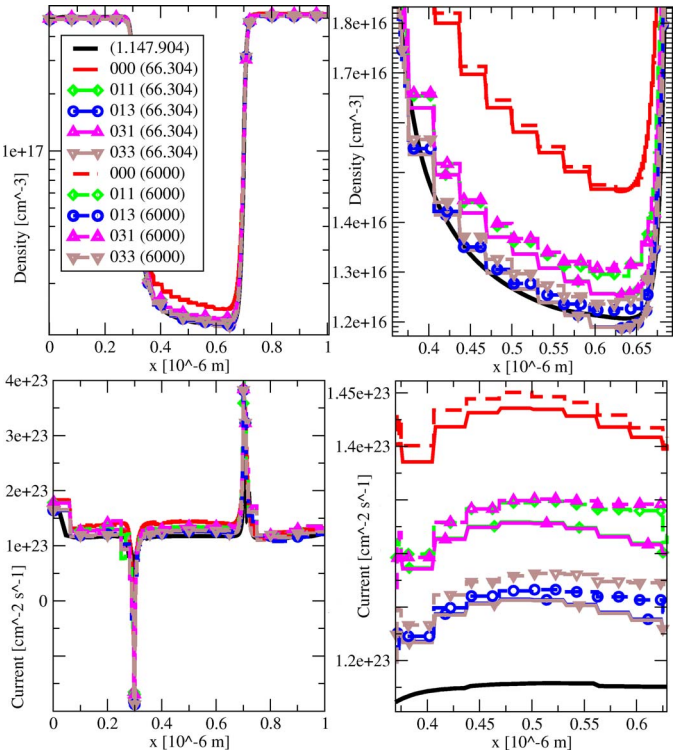


Fig. 6. $n^+nn^+$ simulations at 1V drain with high POs in $\mu$ and $\omega$ directions in analogy to 5.

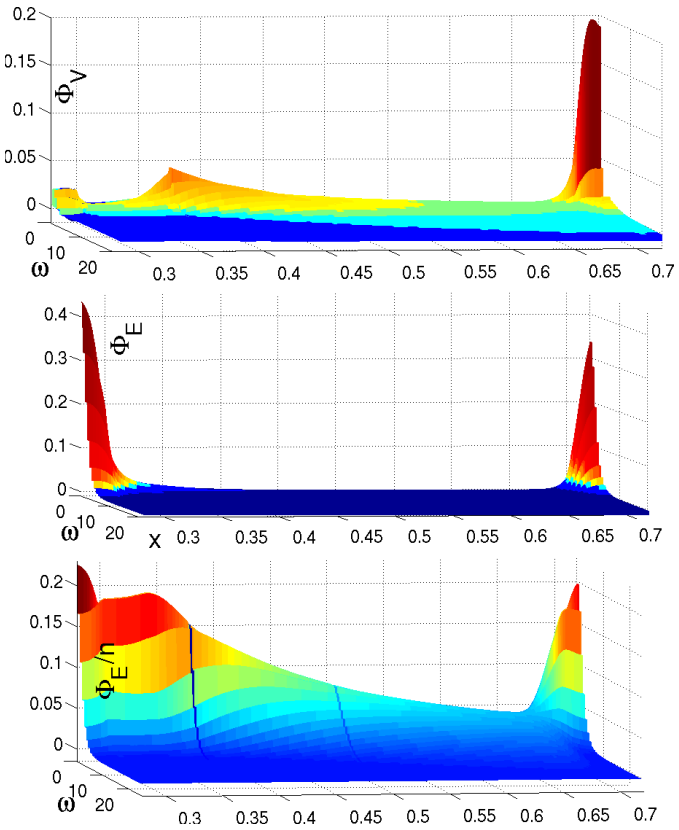


Fig. 7. The Figs. illustrate the phase space separation of the "300 (6000)" simulation at $\mu = 1$, $x = [0.25, 0.75]$ ($n^+n$ junctions are at $x = 0.3$ and $x = 0.7$) and $\omega = [0, 25]$. Top: $\Phi_V$ is partly even larger in the channel region than in the left contact region. Middle: $\Phi_E$ ranges over many orders of magnitude. Bottom: Adaptation for $\Phi_E$ should be based on $\frac{\Phi_E}{n}$.

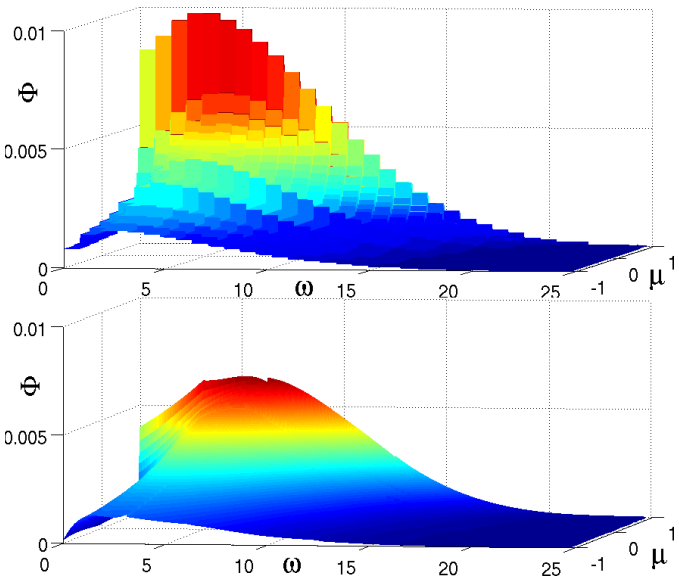


Fig. 8. The Figs. show the "000 (6000)" (upper panel) and "033 (6000)" (lower panel) simulations at $x = 0.6\mu m$.

## References


[1] V. Peikert and A. Schenk, *A Wavelet Method to Solve High-dimensional Transport Equations in Semiconductor Devices*, Proc. 11th Int. Conf. on Simulation of Semiconductor Processes and Devices (SISPAD), Osaka, Japan, Sep. 8 - 10, 2011, pp. 299 - 302.

[2] B. Alpert, *A Class of Bases in $L_2$ for the Sparse Representation of integral Operators*, SIAM Journal on Mathematical Analysis, 1993, 24, pp. 246 - 262.

[3] W. Sweldens, *The Lifting Scheme: A Construction of Second Generation Wavelets*, Applied and Computational Harmonic Analysis, 1996, 3, pp. 186 - 200.

[4] A. Shelton, *A Multi-Resolution Discontinuous Galerkin Method for Unsteady Compressible Flows*, 2008, PhD Thesis, Georgia Institute of Technology, Atlanta.

[5] Y. Cheng, I. M. Gamba and A. Majorana and C.-W. Shu, *A discontinuous Galerkin Solver for the Boltzmann-Poisson System in Nano Devices*, Comput. Methods Appl. Mech. Engrg., 2009, 198, pp. 3130 - 3150.

[6] H.-J. Bungartz and M. Griebel, *Sparse Grids*, Acta Numerica, 13, pp. 147269, May 2004, Cambridge University Press.

[7] G. Widmer, R. Hiptmair and C. Schwab, *Sparse Adaptive Finite Elements For Radiative Transfer*, Journal of Computational Physics, 2008, 227, pp. 6071 - 6105.

[8] C. Jungemann, A.T. Pham, B. Meinerzhagen, C. Ringhofer and M. Bollhofer, *Stable Discretization of the Boltzmann Equation Based on Spherical Harmonics, Box Integration, and Maximum Entropy Dissipation Principle*, Journal of Applied Physics, 2006, 100, pp. 024502-1 - 024502-12.

[9] Sentaurus Device User Guide, Version F-2011.09, September 2011, SYNOPSYS corp.